Atmospheric Environment 45 (2011) 6820–6827

Contents lists available at ScienceDirect

Atmospheric Environment

journal homepage: www.elsevier.com/locate/atmosenv

CVPS: An operator solving complex chemical and vertical processes simultaneously with sparse-matrix techniques

Jinyou Liang [a,*], Mark Z. Jacobson [b]

[a] Air Resources Board, P.O. Box 2815, California Environmental Protection Agency, Sacramento, CA 95814, USA
[b] Department of Civil and Environmental Engineering, Stanford University, Stanford, CA 94305, USA

ARTICLE INFO

Article history:
Received 10 April 2010
Received in revised form
17 November 2010
Accepted 17 December 2010

Keywords:
Ozone
Atmospheric boundary layer
Air quality model
Complex operator
Computer simulation

ABSTRACT

We present a locally, one-dimensional operator that couples complex Chemical and Vertical Physical processes with Sparse-matrix techniques (CVPS) for multi-dimensional regional photochemical transport models. The CVPS operator solves fundamental interaction between chemical reactions and vertical physical processes in the atmospheric boundary layer at each time step, and may be used to simulate chemicals sensitive to both vertical mixing and photochemistry at a time step. The CVPS operator is numerically stable and computationally efficient in atmospheric boundary layers over California. The computational advantage originates from sparse-matrix techniques and the low frequency for communicating feedbacks between CVPS and other local operators. Based on surface Ox ($O_3 + NO_2$) simulations in the Southern California Air Quality Study domain (Harley et al., 1993; Jacobson et al., 1996) on a dual quad-core Linux processor, the ratio of simulation/computer times may reach two for three-dimensional modeling using a classic horizontal advection solver and the CVPS operator.

1. Introduction

Photochemically-reactive species concentrations change rapidly in time and space due to physical and chemical processes in the atmospheric boundary layer, especially near the surface where emissions, deposition, dispersion and photochemical reactions occur simultaneously (Jacobson, 2005; Zhang, 2008). The first attempt to simulate diurnal changes of surface mixing ratios of ozone and its precursors in response to meteorological and emission changes in the atmospheric boundary layer was made by Reynolds et al. (1973). Since then, Eulerian three-dimensional atmospheric models have been improved to simulate a spectrum of atmospheric composition and their interactions over the globe with more detailed representations of chemical and physical processes (e.g., Jacob et al., 1993; Jacobson et al., 1996; Liang and Jacob, 1997; Wang et al., 1998; Mickley et al., 1999; Jacobson, 2001; Li, 2003; Grell et al., 2005), including with optimization techniques (Jacob et al., 1993; Jacobson and Turco, 1994; Jacobson, 1998; Liang and Jacobson, 1999).

It is well known that carefully implemented coupled approaches produce better approximations to the solution of a general system of differential equations than operator splitting methods. Ideally, one would aspire to solve every process in a coupled fashion. However, limitations arising from current CPU time availability make these approaches impractical in most cases (Jacobson, 2005). Chemical changes during a time step may be updated with split operators for complex photochemical transport systems in conjunction with a coupled operator for simple systems in air quality models. While operator-splitting techniques were often applied in large-scale atmospheric modeling studies, techniques that couple at least some processes were preferred, e.g., for investigating responses of air pollutants to emission controls on the regional scale (McRae et al., 1982; Yamartino et al., 1989; Hundsdorfer and Verwer, 2003; Jacobson, 2005). For example, atmospheric advection in three-dimensional chemical transport models has been simulated with locally one-dimensional operators, and vertical physical processes, with one or more operator(s) (Yamartino et al., 1989; Chang et al., 1997; U.S. EPA, 1999; ENVIRON, 2010). These physical operators were separate from locally zero-dimensional chemical operator that could consume most computer time in three-dimensional simulations, where the frequency required for feedbacks among split operators was often much larger for chemical and vertical processes than for horizontal advection in atmospheric boundary layer in typical regional air quality modeling. The significant difference in the required frequency for feedbacks poses a problem in model implementation for general applications. This problem is enhanced for sensitive photochemical compounds in urban boundary layers where vertical mixing time

* Corresponding author. Tel.: +1 916 327 8543; fax: +1 916 322 4357.
E-mail addresses: jliang@arb.ca.gov, jinyou.liang@gmail.com (J. Liang).

1352-2310/$ – see front matter © 2010 Elsevier Ltd. All rights reserved.
doi:10.1016/j.atmosenv.2010.12.035

steps are as short as the e-folding lifetime of many intermediately reactive chemicals in a grid box, though the integration of chemical species changes is typically conducted with sufficiently short sub time step while the bulk air mass is assumed constant at the value solved for by other operators or independent models.

To alleviate the above problem, we introduce a locally one-dimensional operator (CVPS) to solve gas-phase chemical and vertical physical processes simultaneously with sparse-matrix techniques, which improves accuracy for some reactive species and allows for lower frequency than other operators for communicating feedbacks in typical air pollution applications (e.g., Livingstone et al., 2009). The CVPS operator is constructed in the framework of SMVGEAR and NEWRAF (Jacobson and Turco, 1994; Liang and Jacob, 1997; Jacobson, 1998; Liang and Jacobson, 1999; Horowitz, 2006), which have been widely used in atmospheric chemical transport models (e.g., Fiore et al., 2009; Livingstone et al., 2009). The formulation of the CVPS operator will be described first. Then, the implementation of the CVPS operator will be evaluated for numerical stability and computational efficiency. Finally, a preliminary application on surface Ox ($O_3 + NO_2$) will be illustrated.

2. Formulation of the CVPS operator

Atmospheric change of an inert species, such as oxygen or water (A), in a grid box at a time step due to advection, diffusion, chemistry, emission, and deposition processes may be described as

$$\frac{\partial A}{\partial t} = u\cdot\nabla A + \nabla\cdot(K\nabla A) + R(A) + E + D \tag{E0}$$

For N interactive chemical species, atmospheric changes ($\Delta\mathbf{N}$) at a time step ($\Delta\mathbf{t}$) may be simulated with multidimensional models with locally (split, coupled) lower-dimensional operators, as described with equations (E1) and (E2).

$$\Delta\mathbf{N}/\Delta\mathbf{t} = \left[(d\mathbf{N}/d\mathbf{t})_1 + (d\mathbf{N}/d\mathbf{t})_2 + \cdots + (d\mathbf{N}/d\mathbf{t})_n\right] + \left[(\partial\mathbf{N}/\partial\mathbf{t})_1 + (\partial\mathbf{N}/\partial\mathbf{t})_2 + \cdots + (\partial\mathbf{N}/\partial\mathbf{t})_m\right] \tag{E1}$$

In equation (E1), $\Delta\mathbf{N}$ denotes the change of a vector of chemical compounds during a synchronization time step $\Delta\mathbf{t}$. $d\mathbf{N}/d\mathbf{t}$ denotes the rate of change of chemical species in operators $1-n$ that involves time only, and $\partial\mathbf{N}/\partial\mathbf{t}$ involves time and space. The operators in equation (E1) are split, solved one after another using results from previous operator for the same time period, in model implementations. For example, in the U.S. EPA CMAQ (U.S. EPA, 1999; Byun and Schere, 2006), $m=4$ and $n=3$ in a configuration that solves chemical transport changes due to (horizontal, vertical) (advection, diffusion) and chemistry in the gas, aerosol, and aqueous phases (Livingstone et al., 2009). Emission and deposition were merged with vertical diffusion.

$$\Delta\mathbf{N}/\Delta\mathbf{t} = (\delta\mathbf{N}/\delta\mathbf{t})_{1,2,\ldots k} \tag{E2}$$

In equation (E2), processes $1-k$ are solved simultaneously (coupled). The rate of change of chemical species due to processes is denoted with a uniform symbol ($\delta\mathbf{N}/\delta\mathbf{t}$) despite the fact that some of them involve time only in model implementations. Other symbols are the same as in equation (E1).

To simulate surface oxidants, we introduce a locally one-dimensional operator, named CVPS, which couples complex chemical and vertical physical processes, in the planetary boundary layer with sparse-matrix techniques described in Jacobson and Turco (1994). The CVPS operator contains at least one process from each term in the RHS of (E0), as described in (E3). Changes in chemical concentration ($\Delta\mathbf{N}$) during a time step ($\Delta\mathbf{t}$) due to chemistry and vertical physical processes, which include emission, deposition, vertical diffusion and advection, are updated with an iterative Newton–Raphson method (Liang and Jacobson, 1999) in the framework of SMVGEAR with extensions to include a radiative transfer solver for coupled gas-aqueous photochemistry in the troposphere (Jacobson and Turco, 1994; Liang and Jacob, 1997). Following notations in Liang and Jacobson (1999), the partial derivative matrix ($\mathbf{J}$) of the CVPS operator is denoted in equations (E4), (E5) where each pair of (i, j) in the left hand sides denotes a square matrix with i and j in the range of atmospheric boundary layers.

$$\frac{\Delta\mathbf{N}}{\Delta\mathbf{t}} = \frac{d\mathbf{N}}{d\mathbf{t}_{\text{chem}}} + E + D + \frac{\partial}{\partial z}\left(K\frac{\partial N}{\partial z}\right) + w\frac{\partial N}{\partial z} \tag{E3}$$

$$J_{ii,\text{cvps}} = J_{ii,\text{chem}} + J_{ii,\text{D}} + J_{ii,\text{vdiff}} + J_{ii,\text{vadv}} \tag{E4}$$

$$J_{ij,\text{cvps}} = J_{ij,\text{vdiff}} + J_{ij,\text{vadv}} \tag{E5}$$

In equations (E3)–(E5), E and D denote the change of chemical compounds due to emission and deposition processes, and subscripts (chem, vdiff, vadv) denote processes in (chemical reactions, vertical diffusion, vertical advection). Subscripts (ii, ij) denote (diagonal, non-diagonal) matrix–matrix terms specific to boundary layers. $J_{ii,\text{chem}}$ denotes the partial derivative matrix for chemical reactions in layer i that is usually sparse, and all other terms on the right hand side of equations (E4) and (E5) consist of one or more diagonal matrix with the same dimension as $\boldsymbol{J}_{ii,\text{chem}}$.

In the CVPS operator, the dimension of vector $\mathbf{N}$ is the number of simulated chemical species times the number of model layers which just enclose boundary layer. Though equation (E5) allows for both local and non-local closures, the CVPS operator includes only local closure for diffusion and advection with Euler-backward, implicit, finite volume formulation. The algorithm of the CVPS operator ensures the convergence of the finite difference equation from (E3) by using constant (K, w, $\mathbf{z}$) during $\Delta\mathbf{t}$, which is significantly larger with the CVPS operator than without the CVPS operator for simulating surface oxidant in the atmospheric boundary layer over Los Angeles. For example, $\Delta\mathbf{t}$ corresponds to the smaller of the typical lifetime of air parcel in boundary layer and the maximal time step allowed for horizontal operators when the CVPS operator is used, which is over an order of magnitude larger than when the CVPS operator is not used.

3. Validation of the CVPS operator

The CVPS operator was implemented as a standalone library of a locally one-dimensional operator, which may be linked to other necessary components, such as a horizontal advection solver from Yamartino et al. (1989) or others (Walcek, 2000; Byun and Lee, 2002), to form a three-dimensional model. The implementation of the CVPS operator was examined from perspectives of numerical stability and computational efficiency. A preliminary application of the CVPS operator linked to a classic transport package (Yamartino et al., 1989), which was evaluated in Walcek (2000) for the horizontal advection solver, in three-dimensional simulations is also discussed below.

3.1. Implementation of the CVPS operator

The implementation of the CVPS operator was examined in two ways: (1) against its corresponding operator with dense-matrix methods, and (2) against its corresponding split operators.

For the first examination, the CVPS operator was compared with its corresponding operator without sparse-matrix techniques for 1-h O_3 distributions over the greater Los Angeles area in three-dimensional

simulations (Fig. 1). It is shown that the known, significant NOx disbenefit to 1-h O_3 in downtown Los Angeles was prominent after 50 hours of simulation, and simulated 1-h O_3 fields agreed with each other. Hence, the numerical coupling of oxidants between chemical reactions and vertical physical processes in atmospheric boundary layers over the greater Los Angeles area was strong enough to allow for computationally efficient implementation of the CVPS operator.

For the second examination, model simulations with the CVPS operator and split operators were compared for ozone in the vicinity of Los Angeles, California, during August 26–28, 1987, as shown in Fig. 2. It is shown that areas with high 1-h O_3 mixing ratio at 250 m were a little larger than at 10 m. However, differences in oxidant concentrations increased significantly after two days of simulation between the CVPS operator and split operators which treat O_3 and its precursors independently in the formulation. The synchronization time step of 2–5 min is short for the CVPS operator but probably too long for its corresponding split operators due to rapid interactions between O_3 and its anthropogenic precursors. It follows that, at the same synchronization time step of a few minutes, the CVPS operator may significantly improve the precision of simulated oxidant concentration in atmospheric boundary layer when each cell volume is ideally mixed. If not, split operators may represent certain range of observational conditions. When the same amount of computer time was used, CVPS could improve the

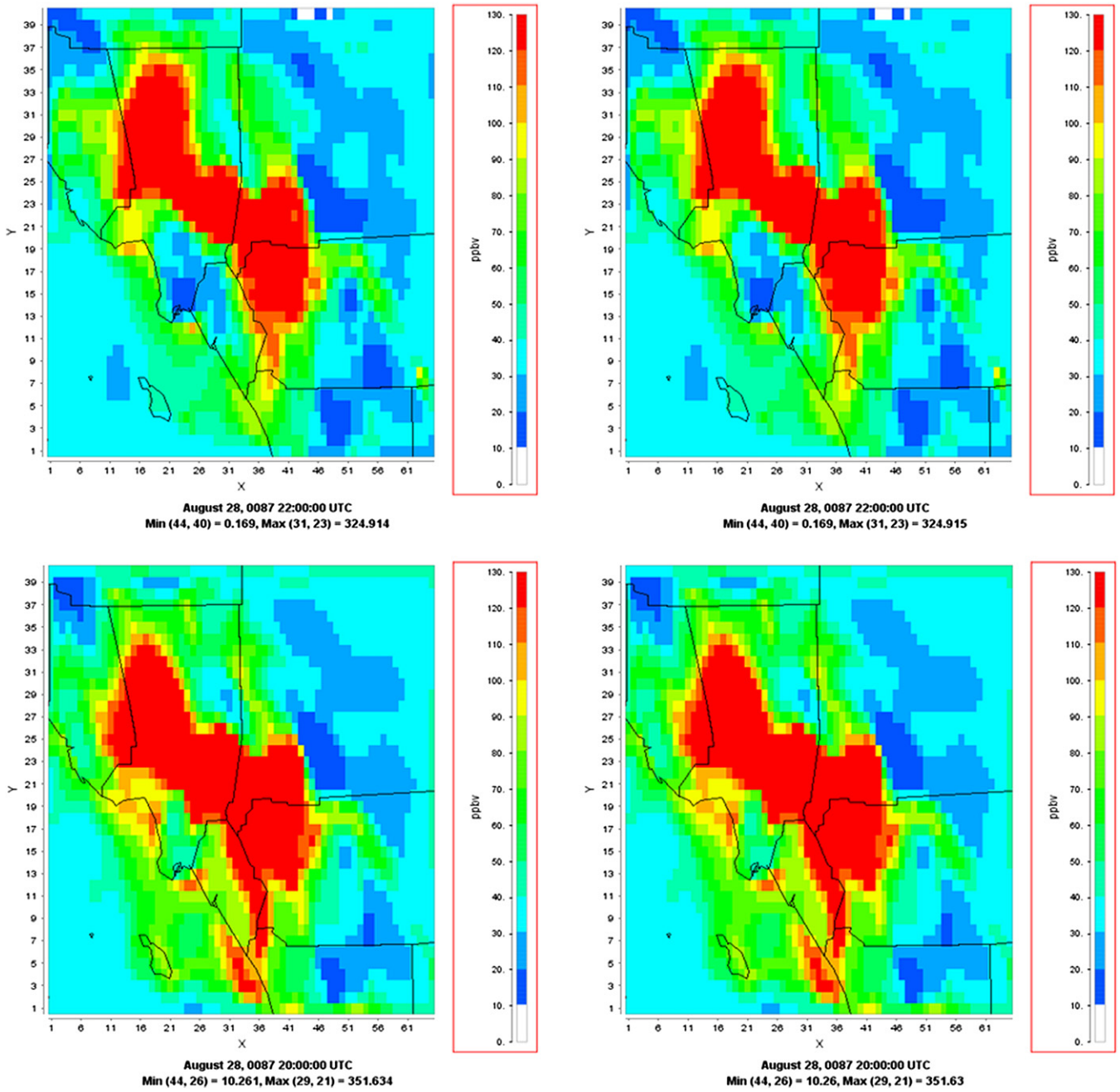

Fig. 1. Simulated O_3 over the greater Los Angeles area at 10 m (top panels) and 250 m (bottom panels) above the surface using a hypothetical emission level in 2005. The CVPS method was implemented without sparse matrix techniques (left) and with sparse matrix techniques (right).

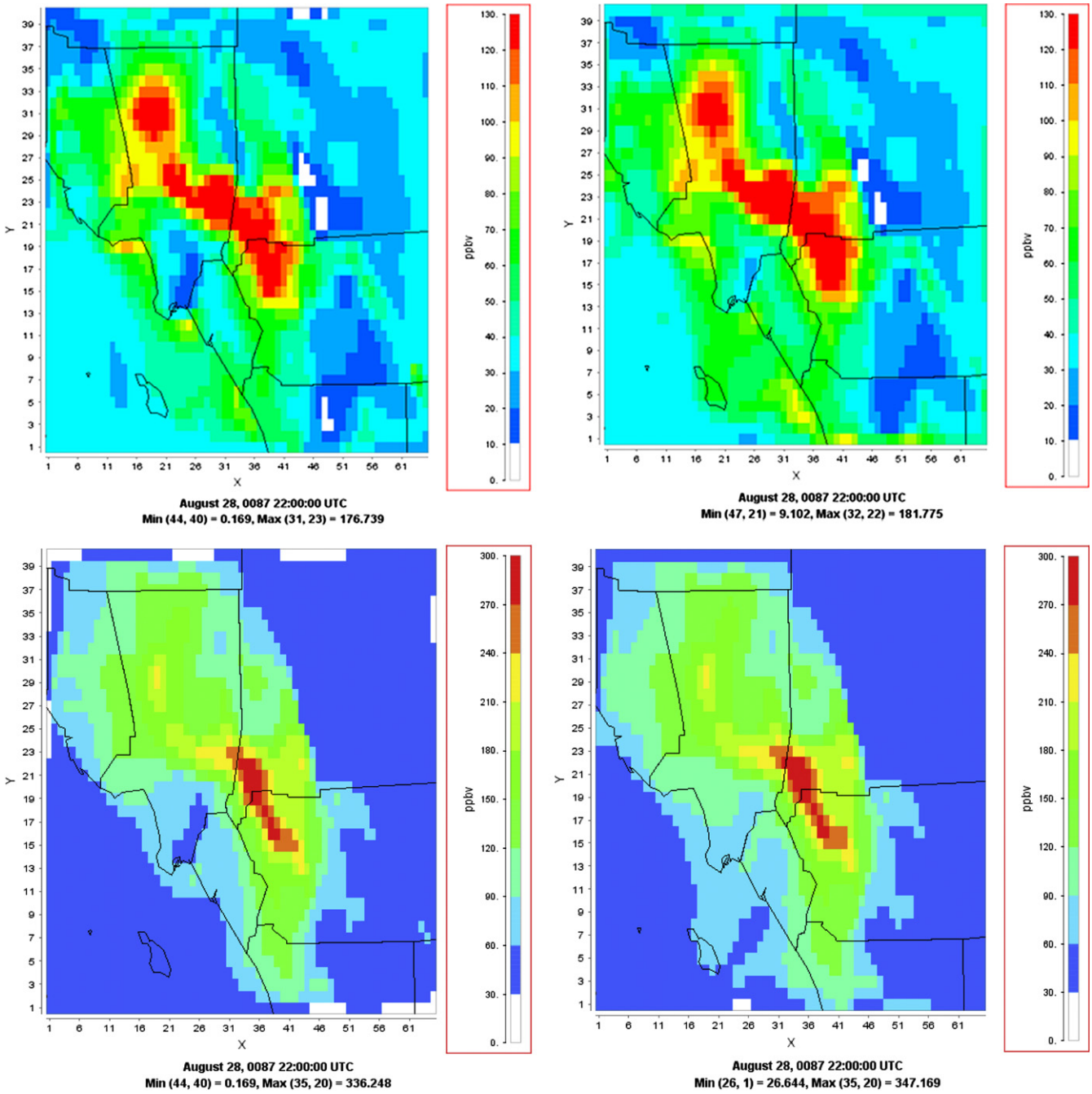

Fig. 2. Simulated O_3 over the greater Los Angeles area at 10 m (left) and 250 m (right) above the ground on August 28, 1987, with the CVPS operator (top) and its corresponding split operators (bottom).

precision for O_3 by 10–260% but only 5–20% for Ox ($=O_3 + NO_2$) in the boundary layer over Los Angeles, as shown in Table 3.

3.2. Numerical stability

The numerical stability of the CVPS operator was tested with increasingly difficult examples for a range of chemical and physical conditions including: (1) a linear chemistry in two thin layers, (2) the carbon-bond chemistry in multiple-column simulations, and (3) an O_3 episode in the greater Los Angeles area. In all simulations, the convergence criteria was 0.1% for all chemical species in all layers and the precision of vertical physical processes were compared with other methods.

The first test was designed to be extremely simple, and contains a linear chemistry in two layers of 20 m thickness. Simulations were conducted to validate the implementation of vertical physical processes (E3) in the CVPS operator. The vertical physical processes in the CVPS operator were computed at the interface of the two adjacent layers, similar to CMAQ (U.S. EPA, 1999; Byun and Schere, 2006), for vertical eddy diffusion and advection. Table 1 lists the initial condition (a) and test results (b). Table 1 shows that, in 5 s, CO concentrations in the two thin layers changed from (1.82, 1) to

(1.56, 1.26) g m^{-3}. The solution was stable and mass conserved to within 0.1% during the iteration, whether the Courant number for diffusion was used or not. The vertical profile, albeit of two layers, was the same as various combinations of split operators. Tested split operators include the chemical solver in the CVPS and the 1-D coupled (diffusion, advection, emission, deposition) solver of the CALGRID model (Yamartino et al., 1989). Due to the overhead of the CVPS operator, split operators performed much faster for this simple problem on a dual quad-core Linux computer.

The second test of the CVPS operator was designed to examine the robustness of the coupling between chemistry and physical processes. Simulations were conducted on a unique terrain of Los Angeles and its neighboring counties. There were (65×40) columns in the simulations, and each column extended to the diffusion break from a surface area of (5 km $\times$ 5 km). The number of model layers containing the atmospheric boundary layer varies, but the layer thickness was constant in the simulations. The Carbon Bond Mechanism (Gery et al., 1989; Liang and Jacobson, 2000) was used. The vertical diffusivity ranged from 10–120 m^2 s^{-1} and the atmospheric boundary layer extended 3–7 vertical model layers. Table 2 lists initial conditions and test results. Initial chemical environment mimics a smog-chamber experiment, while the physical environment is similar to Los Angeles area. Photolysis rates were calculated for each layer in each column during a widely studied period conducive for high 1-h ozone formation. Table 2(b) shows that, in the hypothetic conditions, 1-h O_3 in the bottom layer increased from 33 ppbv at 6 am to ~780 ppbv at 6 pm with peak up to ~820 ppbv at 4 pm. Difference within a row reflects geographic effect, and difference in a column except the last cell was due to vertical mixing conditions. When vertical physical processes were turned off, the 1-h O_3 was slightly lower. The last row shows the effect of additional OH source, as reported by Li et al. (2008), which reduced peak 1-h O_3 in the bottom layer in contrast to the case reported by Wennberg and Dabdub (2008) presumably due to different chemical scheme used here.

The final test of the CVPS operator was conducted with three-dimensional simulations using an observed O_3 episode in the greater Los Angeles area, to examine potential constraints of vertical advection and diffusivity on iteration time steps in the Newton-Raphson method without a Courant number and with Courant numbers of 0.2 and 0.5, respectively. As the sub time step used in chemical integration was relatively small and vertical diffusion dominated in the atmospheric boundary layer over Los Angeles in the simulations, the effect of Courant numbers was small, similar to that in the first case. The effect of various synchronization time steps, with values of (10, 5, 2.5) minutes, respectively, was also examined in this test (last three rows of Table 3). As the chemical lifetime of surface air parcels against vertical transport near the diffusion break is on the order of an hour or longer over California,

Table 1
Test of the CVPS operator on an ideal case.

(a) Initial conditions			
Variable	Unit	Layer 1	Layer 2
CO[a]	g m^{-3}	1.82	1
P	hPa	1013.25	1011.22
T	K	303.15	303
D	m s^{-1}	0.01	0
E	g m^{-3} s^{-1}	2.37×10^{-08}	0
K_{zz}	m^2 s^{-1}	50	0
W	m s^{-1}	0.01	0
Thickness	m	20	20
dt	s	5	5
(b) Final CO concentration (g m^{-3})			
Cw*	Cvd*	Layer 1	Layer 2
0.05	0.0005	1.56	1.26
0.002	0.005	1.56	1.26
0.02	0.05	1.56	1.26
0.05	0.1	1.55	1.27
0.05	0.2	1.56	1.26
0.05	0.3	1.56	1.25
0.05	0.4	1.56	1.26
0.05	0.5	1.56	1.26
NA	NA	1.56	1.26

[a] CO is assumed to decay at a rate due to its reaction with hydroxyl radical with constant concentration of 4×10^6 molecules cm^{-3}. *Cw and Cvd denote Courant numbers for vertical wind (W) and eddy diffusion (K_{zz}), respectively. 'NA' denotes 'not applied'.

Table 2
Test of the CVPS operator with multi-column simulations.

(a) Initial condition	
Species	Initial value (ppbv)
HCHO	3.77
NO_2	19.80
O_3	29.60
CH_3CHO	1.46
C_2H_4	491
OLE	0.301
PAR	14.80
Tolune	0.06
Xylene	0.04
CO	309
NO	177
T (K)	300
P (atm)	1
H_2O (g m^{-3})	8
Photolysis	6 am–6 pm, 8/26/1987

(b) Bottom layer ozone in various simulations				
Ozone	Los Angeles	Orange	Riverside	San Bernardino
(N7, K120)[a]:				
Noon	260	258	241	236
6 pm	801	802	803	802
Peak (hour)	818 (4 pm)	820 (4 pm)	819 (4 pm)	818 (4 pm)
(N7, K50)[a]:				
Noon	258	256	239	235
6 pm	801	802	803	802
Peak (hour)	817 (4 pm)	819 (4 pm)	819 (4 pm)	817 (4 pm)
(N3, K10)[a]:				
Noon	215	214	200	196
6 pm	781	783	784	782
Peak (hour)	795 (4 pm)	797 (4 pm)	796 (4 pm)	794 (4 pm)
(N0, K0):				
Noon	209	208	194	190
6 pm	778	780	781	780
Peak (hour)	792 (4 pm)	794 (4 pm)	794 (4 pm)	791 (5 pm)
(N0, K0)[b]:				
Noon	759	759	758	757
6pm	717	717	717	718
Peak (hour)	764 (1 pm)	764 (1 pm)	764 (1 pm)	764 (1 pm)

Each value represents an average of 1-h O_3 in the bottom layer of all columns over the terrain of a county. Difference in a row reflects geographic effect, and difference in a column except the last one was due to vertical mixing conditions.

[a] (N7, K120) denotes that the atmospheric boundary layer extended seven model layers with thickness of 20 m at the bottom, and the vertical diffusivity (Kzz) was 120 m^2 s^{-1} in the bottom layer; Kzz was specified with an incrementally smaller value (by 5) at higher layers until the diffusion break. (N7, K50) and (N3, K10) follow the same convention. (N0, K0) denotes box model simulations.

[b] The additional OH source, as described in Li et al. (2008) and Wennberg and Dabdub (2008), was included. See text for more information.

the effects were dominated by the horizontal advection operator (Walcek, 2000; Byun and Lee, 2002).

3.3. Computational efficiency

The CVPS operator may gain computational advantage over corresponding split operators for two reasons: (1) the use of sparse-matrix techniques, and (2) the low frequency required to communicate with other operators.

The sparseness of the partial derivative matrix (E4) and (E5) for a column of atmospheric boundary layer is significant in the CVPS, even when a dense chemical mechanism is used. Without sparse-matrix techniques, the CVPS operator would increase the calculation of matrix inversion by a factor on the order of $N(N^2-1)$ from the locally, zero-dimensional operator; where N denotes the number of model layers enclosing atmospheric boundary layer. Sparse-matrix techniques dramatically reduced the computer time for a locally, zero-dimensional operator with various photochemical mechanisms. In the CVPS operator, sparse-matrix techniques yielded similar savings of computer time. For example, when atmospheric boundary layer was enclosed in two model layers, sparse-matrix techniques reduced matrix inversion calculations by 77% for a version of carbon-bond photochemical mechanism.

Three-dimensional modeling with the CVPS operator can afford relatively low frequency for communicating feedbacks between the CVPS operator and other operators that represent vertical transport processes in free troposphere and horizontal transport processes in the atmosphere. The dependences of the CVPS operator and its corresponding split operators on synchronization time steps were evaluated with a number of 1-h three-dimensional simulations over the greater Los Angels area during 10–11 am on August 26, 1987, using reduced emission levels corresponding to a recent year (2005). As the horizontal advection solver is not in the CVPS operator, a classic horizontal advection solver (Yamartino et al., 1989) was used; more up-to-date horizontal advection solvers (Walcek, 2000; Byun and Lee, 2002) may be used in future applications. Synchronization time steps of (10, 5, 2.5) minutes were conducted for the CVPS operator, and incrementally shrinking synchronization time steps ranging from 5 min to 4.7 s were conducted for the corresponding split operators. Table 3 lists computer time for various synchronization time steps vs. simulated concentrations (ppbv) of 1-h O_3 and Ox. It is shown that both the CVPS operator and its corresponding split operators converged on their own, but the difference between the two methods remains. This difference originated from the coupling nature of individual processes included in the CVPS operator for major oxidant (Ox). For example, when significant amount of NO was emitted and the operator that contains emission is calculated after the chemistry operator in the split method, O_3 from the CVPS method is expected to be lower than from the split method due to its titration by NO. Thus, the difference between the two methods in simulated oxidant concentration was smaller for Ox than for O_3.

4. Preliminary application on surface Ox

The CVPS operator was linked to a classic horizontal advection solver (Yamartino et al., 1989), which was shown to have reasonable performance for advecting urban tracers (Walcek, 2000), and applied to assess the success of air pollution mitigation measures for reducing surface Ox over Los Angeles during 1975–2005.

Based on results presented in previous section, the CVPS operator yielded significantly more accurate O_3 simulation than its counterpart split operators when the grid volume is ideally mixed. However, the improved accuracy from the use of the CVPS operator is not expected to be as large as the spatial and temporal variations of emission and meteorological fields which are often insufficient for reproducing chemical datasets. In addition, regional air quality modeling has relatively coarse spatial resolution even in California where substantial efforts have been conducted for data acquisition and model analysis (http://www.arb.ca.gov/airways/ccaqs.htm), and the existing emission inventories and profiles are in continual development (http://www.arb.ca.gov/ei/ei.htm). To compare with observed values of many chemical compounds, regional air quality models that currently have resolutions of ($\sim$5 km $\times$ $\sim$5 km) horizontally and ($\sim$30 m) vertically near the surface likely need to be linked to neighborhood-scale models, models of room air, and models for human exposures, or need to use various evaluation methods (Livingstone et al., 2009), which are out of the scope of this paper. However, the difference between the two methods was within 20% for Ox in boundary layers over Los Angeles. Thus, we reserve results of single oxidants for future applications and discuss Ox results here.

Fig. 3 shows simulated Ox distributions over the greater Los Angeles area at 10 m (left panel) and 250 m (right panel) above the ground, respectively, for two cases. The first case (top panel) corresponds to conditions occurred on August 28, 1987, and the second case (bottom panel) substituted the 1987-emission with hypothetical emissions in 2005 if no air quality mitigation efforts had been applied during 1975–2005 (Motallebi et al., 2009). It is shown that (1) Ox at 250 m level was comparable to that at 10 m level, and (2) Ox in 2005 would be over three times that in the 1987 case at both levels without air pollution mitigation measures during 1975–2005. Therefore, air pollution mitigation measures

Table 3
Simulated surface oxidants and computer timings.

Methods	dt (s)	Clock time (s)	LA(O_3)	OR(O_3)	RS(O_3)	SB(O_3)	LA(Ox)	OR(Ox)	RS(Ox)	SB(Ox)
C:VPS	300.0	147	54.0	53.8	51.8	38.0	68.4	85.3	56.4	40.0
C:VPS	150.0	267	53.5	52.7	51.5	37.9	68.3	85.0	56.3	40.0
C:VPS	75.0	473	52.3	49.5	51.1	37.7	68.9	84.7	56.5	40.0
C:VPS	37.5	853	52.2	49.0	50.8	37.6	69.0	84.6	56.4	40.0
C:VPS	18.8	1541	52.0	48.8	50.6	37.5	68.8	84.4	56.2	40.0
C:VPS	9.4	2845	51.8	48.5	50.4	37.5	68.7	84.2	56.1	39.9
C:VPS	4.7	5215	51.7	48.1	50.1	37.5	68.7	84.0	55.9	40.0
CVPS	600.0	1453	32.3	13.4	41.0	34.4	61.0	69.0	51.3	38.3
CVPS	300.0	1631	32.5	13.5	41.0	34.4	61.2	69.1	51.3	38.4
CVPS	150.0	2536	32.7	13.5	40.9	34.4	61.4	69.2	51.3	38.4

*Surface oxidants (O_3 and Ox) concentrations over counties of Los Angeles (LA), Orange (OR), Riverside (RS) and San Bernardino (SB) were simulated for 10–11 am on August 26, 1987, using the CVPS operator and its corresponding split operators, denoted as C:VPS in the first column, at emission level in 2005. Ten 1-h simulations were conducted with various synchronization time steps (dt) applied for the CVPS operator (10 min, 5 min, 2.5 min) and its corresponding split operators (5 min, 2.5 min, …, 4.7 s), respectively. Clock time reflects computer time used for each simulation under conditions specific to a dual quadcore Linux processor at California Air Resources Board.

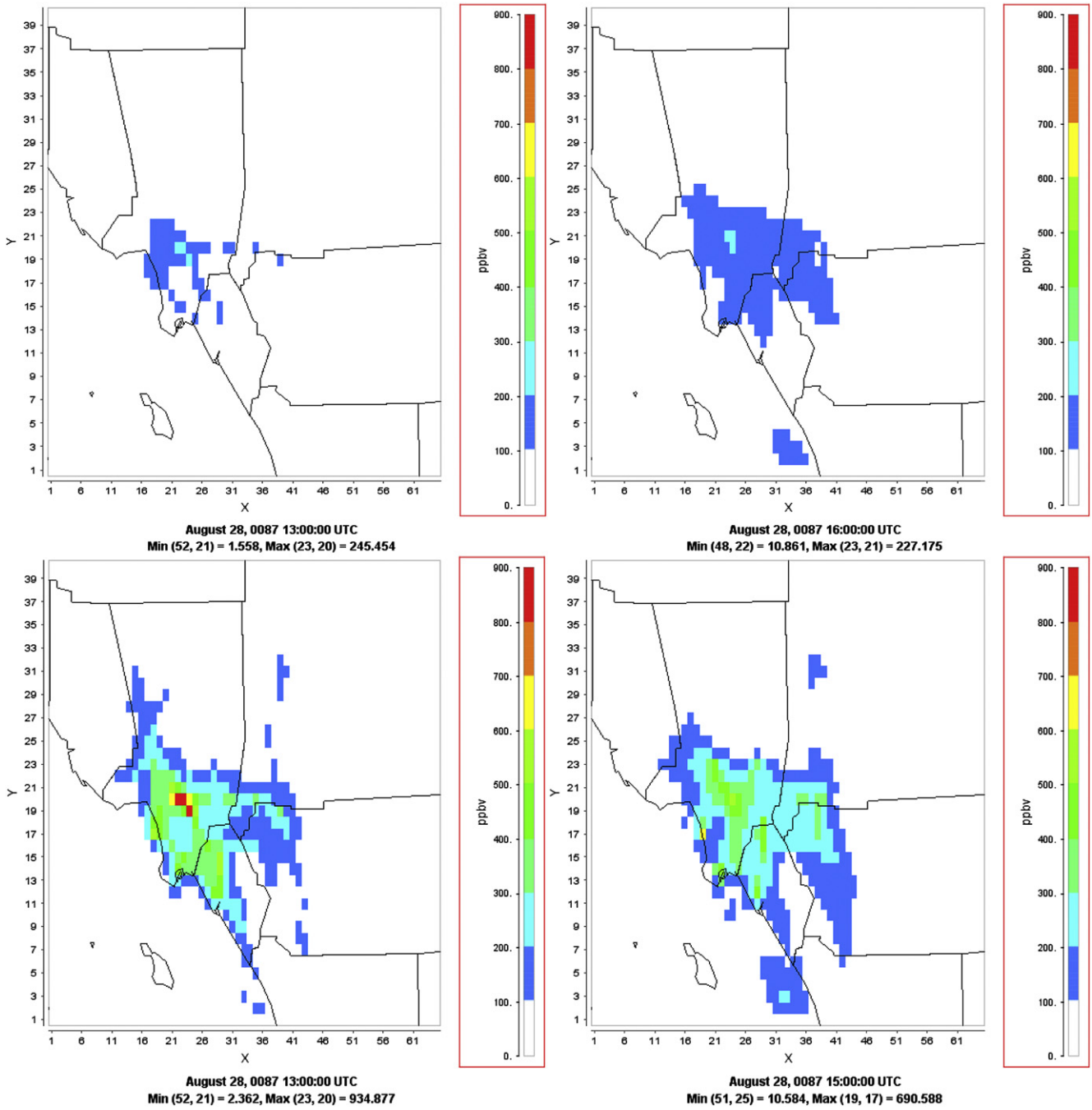

Fig. 3. Simulated distribution of Ox ($O_3 + NO_2$) over greater Los Angeles area at 10 m (left) and 250 m (right) above ground in August 1987 (top) and the '2005-BAU' case (bottom).

during 1975–2005 had greatly reduced surface Ox concentration over Los Angeles in 2005.

5. Conclusion

A locally, one-dimensional operator that couples complex Chemical and Vertical Physical processes with Sparse-matrix techniques (CVPS) for multidimensional regional photochemical transport models was developed. The CVPS operator solves fundamental interactions between gas-phase chemistry and vertical physical processes in the atmospheric boundary layer at each time step, and may be used to simulate chemicals sensitive to both vertical mixing and photochemistry during a time step. The formulation of the operator was described, and the implementation of the operator was evaluated with (a) multiple-column simulations with initial chemical conditions from a smog-chamber experiment, and (b) three-dimensional simulations with inputs from a classic 1-h ozone episode in greater Los Angeles area. The CVPS operator was found numerically stable and computationally efficient in atmospheric boundary layer over California. Difference in simulated surface ozone concentration from using the CVPS operator and its counterpart split operators, which originates from model formulations, was significant in areas with substantial emission of NO, and the corresponding difference was much smaller for Ox. The computational advantage originates from sparse-matrix techniques and the low frequency for communicating

feedbacks between CVPS and other local operators, based on surface Ox simulations in California.

Acknowledgements

We are indebted to: Daniel J. Jacob at Harvard University for discussions from scientific perspectives; Bart Croes, Bruce Jackson, Nehzat Motallebi, Donald Johnson at California Air Resources Board for assistance in SCAQS data analysis and computer system administration.

References

Byun, D.W., Lee, S.M., 2002. Numerical advection of trace species under non-uniform density distribution. In: Chock, D., Carmichael, G. (Eds.), In the IMA volume on Air Quality Modeling.

Byun, D.W., Schere, K.L., 2006. Review of the governing equations, computational algorithms, and other components of the Models-3 Community Multiscale Air Quality (CMAQ) modeling system. Applied Mechanics Reviews 59, 51–77.

Chang, J.S., Jin, S., Li, Y., Beauharnois, M., Lu, C.H., Huang, H.C., Tanrikulu, S., DaMassa, J., 1997. The SARMAP Air Quality Model. Final Report to Air Resources Board, California Environmental Protection Agency. Sacramento, CA.

ENVIRON, 2010. User's Guide to Comprehensive Air Quality Model with Extensions (CAMx): Ozone, Particulates, Toxics. Novato, CA.

Fiore, A.M., 46 coauthors, 2009. Multimodel estimates of intercontinental source-receptor relationships for ozone pollution. J. Geophys. Res. 114, D04301. doi:10.1029/2008JD010816.

Gery, M.W., Whitten, G.Z., Killus, J.P., Dodge, M.C., 1989. A photochemical kinetics mechanism for urban and regional scale computer modeling. J. Geophys. Res. 94, 12,925–12,956.

Grell, G.A., Peckham, S.E., Schmitz, R., McKeen, S.A., Frost, G., Skamarock, W.C., Eder, B., 2005. Fully coupled "online" chemistry within the WRF model. Atmos. Environ. 39, 6957–6975.

Harley, R.A., Russell, A.G., McRae, G.J., Cass, G.R., Seinfeld, J.H., 1993. Photochemical modeling of the Southern California Air Quality Study. Environ. Sci. Technol. 27, 378–388.

Horowitz, L.W., 2006. Past, present, and future concentrations of tropospheric ozone and aerosols: methodology, ozone evaluation, and sensitivity to aerosol wet removal. J. Geophys. Res. 111, D22211. doi:10.1029/2005JD006937.

Hundsdorfer, W., Verwer, J.G., 2003. Numerical solution of time-dependent advection-diffusion-reaction equations. In: Springer Series in Computational Mathematics, vol. 33 Berlin.

Jacob, D.J., Logan, J.A., Yevich, R.M., Gardner, G.M., Spivakovsky, C.M., Wofsy, S.C., Munger, J.W., Sillman, S., Prather, M.J., Rodgers, M.O., Westberg, H., Zimmerman, P.R., 1993. Simulation of summertime ozone over North America. J. Geophys. Res. 98, 14,797–14,816.

Jacobson, M.Z., Lu, R., Turco, R.P., Toon, O.B., 1996. Development and application of a new air pollution modeling system. Part I: Gas-phase simulations. Atmos. Environ. 30B, 1939–1963.

Jacobson, M.Z., 1998. Improvement of SMVGEAR II on vector and scalar machines through absolute error tolerance control. Atmos. Environ. 32, 791–796.

Jacobson, M.Z., 2001. GATOR-GCMM: A global through urban scale air pollution and weather forecast model-1-Model design and treatment of subgrid soil, vegetation, roads, rooftops, water, sea ice, and snow. J. Geophys. Res. 106, 5385–5402.

Jacobson, M.Z., 2005. Fundamentals of Atmospheric Modeling, second ed. Cambridge University Press, New York, NY.

Jacobson, M.Z., Turco, R.P., 1994. SMVGEAR: A sparse-matrix, vectorized Gear code for atmospheric models. Atmos. Environ. 28A, 273–284.

Li, S., Matthews, J., Sinha, A., 2008. Atmospheric hydroxyl radical production from electronically excited NO_2 and H_2O. Science 319, 1657–1660.

Li, Q., 2003. Intercontinental Transport of Anthropogenic and Biomass Burning Pollution. Ph.D. Dissertation, Harvard University, Cambridge, MA, U.S.A.

Liang, J., Jacob, D.J., 1997. Effect of aqueous-phase cloud chemistry on tropospheric ozone. J. Geophys. Res. 102, 5993–6001.

Liang, J., Jacobson, M.Z., 1999. A study of sulfur dioxide oxidation pathways over a range of liquid water contents, pH values, and temperatures. J. Geophys. Res. 104, 13,749–13,769.

Liang, J., Jacobson, Mark Z., 2000. Comparison of a 4000-reaction chemical mechanism with the Carbon Bond IV and an adjusted Carbon Bond IV-EX mechanism using SMVGEAR II. Atmos. Environ. 34, 3015–3026.

Livingstone, P.L., Magliano, K., Gürer, K., Allen, P.D., Zhang, K.M., Ying, Q., Jackson, B.S., Kaduwela, A., Kleeman, M., Woodhouse, L.F., Turkiewicz, K., Horowitz, L.W., Scott, K., Johnson, D., Taylor, C., O'Brien, G., DaMassa, J., Croes, B.E., Binkowski, F., Byun, D., 2009. Simulating PM concentration during a winter episode in a subtropical valley: sensitivity simulations and evaluation methods. Atmos. Environ. 43, 5971–5977.

McRae, G.J., Goodin, W.R., Seinfeld, J.H., 1982. Mathematical Modeling of Photochemical Air Pollution. Final Report to California Air Resources Board, Sacramento, California, U.S.A.

Mickley, L.J., Murti, P.P., Jacob, D.J., Logan, J.A., Rind, D., Koch, D., 1999. Radiative forcing from tropospheric ozone calculated with a unified chemistry-climate model. J. Geophys. Res. 104, 30,153–30,172.

Motallebi, N., et al., 2009. The Effect of Emission Reductions on Ozone and Fine Particulate Matter Air Quality in California from Business-as-usual Perspective. Research Division, California Air Resources Board, Sacramento, CA, U.S.A.

Reynolds, S.D., Roth, P.M., Seinfeld, J.H., 1973. Mathematical modeling of photochemical air pollution—I: Formulation of the model. Atmos. Environ. 7, 1033–1061.

U.S. EPA, 1999. Science Algorithms of the EPA Models-3 Community Multiscale Air Quality (CMAQ) Modeling System. EPA/600/R-99/030, Washington, DC. Eds. Byun, D.W., Ching, J.K.S.

Walcek, C., 2000. Minor flux adjustment near mixing ratio extremes for simplified yet highly accurate monotonic calculation of tracer advection. J. Geophys. Res. 105, 9335–9348.

Wang, Y., Jacob, D.J., Logan, J.A., 1998. Global simulation of tropospheric O_3-NOx-hydrocarbon chemistry 1. Model formulation. J. Geophys. Res. 103, 10,713–10,726.

Wennberg, P.O., Dabdub, D., 2008. Rethinking ozone production. Science 319, 1624–1625.

Yamartino, R.J., Scire, J.S., Hanna, S.R., Carmichael, G.R., Chang, Y.S., 1989. CALGRID: a mesoscale photochemical grid model. Final Report to California Air Resources Board, Sacramento, CA, U.S.A.

Zhang, Y., 2008. Online-coupled meteorology and chemistry models: history, current status, and outlook. Atmos. Chem. Phys. 8, 2895–2932.